Catalysis Communications 12 (2011) 996–999

Contents lists available at ScienceDirect

Catalysis Communications

journal homepage: www.elsevier.com/locate/catcom

Short Communication

Effect of activation temperature on the surface copper particles and catalytic properties of Cu–Ni–Mg–Al oxides from hydrotalcite-like precursors

Chenghua Xu [*], Liangke Zheng, Danfeng Deng, Jianying Liu, Shengyu Liu

College of Resources and Environment, Chengdu University of Information Technology, Chengdu 610225, PR China

ARTICLE INFO

Article history:
Received 15 October 2010
Received in revised form 5 March 2011
Accepted 8 March 2011
Available online 15 March 2011

Keywords:
Hydrotalcite-like precursors
Cu^0 metal particles
Furfural hydrogenation
Furfuralcohol
2-Methylfuran

ABSTRACT

The Cu–Ni–Mg–Al oxides catalysts for furfural hydrogenation were prepared from the hydrotalcite-like precursors, and the effect of activation temperature on the Cu^0 particles and catalytic properties of the catalyst was thoroughly investigated. The catalyst activated by H_2 at 300 °C was found to exhibit the best catalytic activity, due to the presence of the smallest Cu^0 particles with a high dispersion. Moreover, the bigger Cu^0 particles were active for furfuralcohol hydrogenolysis to 2-methylfuran in the liquid-phase (ethanolic solution), and the hydrogenation of the furan ring of furfuralcohol and 2-methylfuran on Cu^0 particles was easily achieved in the vapour-phase.

© 2011 Elsevier B.V. All rights reserved.

1. Introduction

Furfural (FFR) can be hydrogenated to produce an important chemical, furfuralcohol (FFA), which is mainly used in polymer industry, synthetic fibers, rubber-resins, farm chemical and in other products from fine chemical industry. The commercial catalyst used in the FFR hydrogenation is a Cr_2O_3 promoted Cu-containing catalyst, wherein MgO generally acts as support. Nagaraja et al. [1,2] have studied Cu–MgO coprecipitated catalysts for FFR hydrogenation to FFA in the gas phase and concluded that the presence of both Cu^+ and Cu^0 species was responsible for the high selectivities obtained. The same group has reported the use of a Cu–MgO–Cr_2O_3 catalyst for FFR gas-phase hydrogenation to FFA using cyclohexanone dehydrogenation as hydrogen resource [2]. Their conclusion is that Cr_2O_3 can stabilize the Cu^0/Cu^+ species required for both the hydrogenation/dehydrogenation reactions. However, the toxicity of Cr_2O_3 in Cr_2O_3 promoted Cu-containing catalysts will cause severe environmental pollution. Recently, a Cu–Fe/SiO_2 catalyst has been reported to show a high selectivity towards the FFR hydrogenation to 2-methyfuran via the selective hydrogenolysis of the intermediate FFA [3].

The present work aimed: i) to prepare a new environmentally friendly FFR hydrogenation catalyst ($CuNiMgAlO_y$) with a high Cu dispersion from the hydrotalcite-like precursors according to our previous work [4]; ii) to study thoroughly the effect of activation temperature on the characteristics of Cu^0 species at the catalyst surface such as their dispersion, the metal specific surface area and the particle size; and iii) to investigate the FFR catalytic hydrogenation over this catalyst activated by H_2 at different temperatures both in the liquid and vapour-phase.

2. Experimental

The Cu–Ni–Mg–Al mixed oxides catalysts ($CuNiMgAlO_y$) were prepared by the calcination of the corresponding hydrotalcite-like precursors ($CuNiMgAl(OH)_x$) at 500 °C in air for 4 h. The precursors were synthesized according to the procedure reported in the literature [4], wherein the molar composition of metal ions was $11.2Cu^{2+}:4.7Ni^{2+}:50Mg^{2+}:50Al^{3+}$. The obtained catalysts were characterized by XRD, N_2 adsorption–desorption, XPS, H_2-TPR and H_2–N_2O titration. The Cu surface area (S_{Cu}), dispersions (D_{Cu}) and average particle size (r_{av}) of the reduced catalysts were calculated according to H_2–N_2O titration as the previous reports [5,6]. The FFR liquid-phase and vapour-phase hydrogenation were carried out at 200 and 220 °C, respectively. The catalysts were activated by H_2 in the temperature range of 220–400 °C. The detailed procedures are described in the Supplementary material.

3. Results and discussion

3.1. Textural and structural properties

The XRD patterns of the calcined catalyst ($CuNiMgAlO_y$) and its precursor ($CuNiMgAl(OH)_x$) (Fig. 1) clearly indicate that CuNiMgAl$(OH)_x$ exhibits a typical hydrotalcite-like phase, which will be destroyed to form spinel species such as $MgAlO_2$, $CuAlO_2$ or $NiAlO_2$ [7,8], and even a small number of oxides [9] during the calcination. Meanwhile, the

---

[*] Corresponding author. Tel.: +86 28 85966011; fax: +86 28 85966089.
E-mail address: xch@cuit.edu.cn (C. Xu).

1566-7367/$ – see front matter © 2011 Elsevier B.V. All rights reserved.
doi:10.1016/j.catcom.2011.03.011

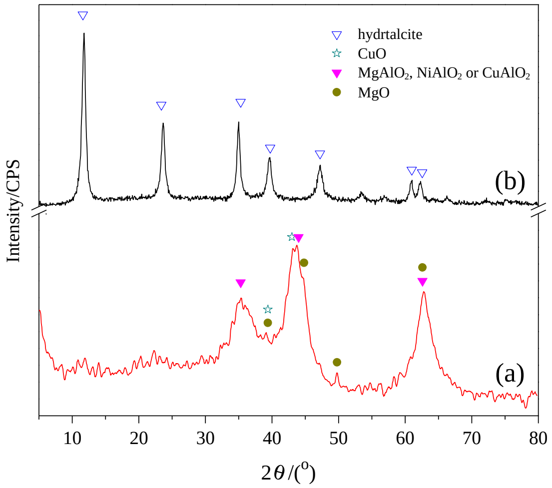

Fig. 1. XRD patterns of the calcined catalyst CuNiMgAlO$_y$ (a) and its precursor (b).

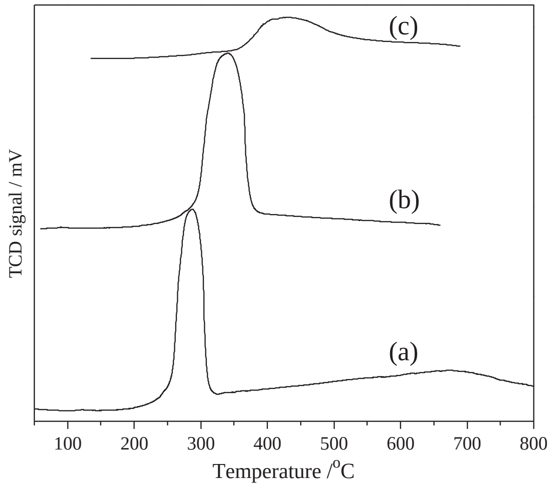

Fig. 2. H_2-TPR profiles of the CuNiMgAlO$_y$ catalyst (a), Cu$_{11.2}$/MgAlO$_x$ (b) and Ni$_{4.7}$/MgAlO$_x$ (c).

characteristic peaks for CuO in CuNiMgAlO$_y$ are very weak and no NiO species are detected, indicating that Cu^{2+} and Ni^{2+} species in CuNiMgAlO$_y$ are mainly located in the spinel phase or highly dispersed onto $MgAlO_2$ or MgO.

The N_2 adsorption–desorption analysis (Fig. S1 in the Supplementary material) shows that the isotherm for catalyst precursor is typical of Type II in nature and exhibits a clear open H_3 hysteresis loop according to the IUPAC classification, which is often recorded in layered materials with long and narrow cleft [10,11]. However, the calcined catalyst gives a close H3 hysteresis loop, indicating that the layered structure of hydrotalcite-like precursor has been destroyed to form a new phase, and its surface area, pore diameter and pore volume (Table 1) are increased after calcination due to the gradual disappearance of the interlay OH^- and CO_3^{2-} anions.

3.2. Surface species and reducibility properties

In the previous studies [1,2,12], the Cu^0 species were considered to be the catalytic active centers for FFR hydrogenation over the Cu-containing catalysts. The H_2-TPR results of catalysts (Fig. 2) show that CuNiMgAlO$_y$ gives an intensive H_2 consumption peak at 287 °C and a weak peak at about 675 °C. The former can be ascribed to the reduction of the highly dispersed Cu^{2+} species including the isolated Cu^{2+} ions in spinel and CuO [8], the latter one is assigned to the reduction of Ni^{2+} species. Moreover, it can also be observed that the Cu^{2+} species in catalyst from hydrotalcite-like precursors are reduced more easily than those in Cu-supported catalyst, however the Ni^{2+} species are difficultly reduced in comparison to those in the supported Ni catalyst. It is possibly due to the bigger ionic radius of Cu^{2+} (0.073 nm) than that of Ni^{2+} (0.069 nm), resulting in the migration of Cu^{2+} cations to the surface spinel phase to form the highly dispersed CuO phase and the easy penetration of Ni^{2+} species into the bulk phase, which has been proved by the above XRD results.

The XPS analysis of catalysts activated by H_2 at different temperatures (Fig. 3) shows that the intensity of peaks at 932.4 eV, assigned to the characteristic Cu2p$_{3/2}$ binding energy values of metallic copper [13], is increased with the rise of activation temperature, however the peak at 933.8 eV ascribed to Cu^{2+} species almost disappears at the activation temperature of 300 °C. Therefore, the Cu^{2+} species in the catalyst are deduced to be completely reduced by H_2 to Cu^0 when the activation temperature is beyond 300 °C.

Table 1
Textural characteristics for the calcined catalyst and its precursor.

Catalysts	Most probable pore diameter (nm)	BET surface area ($m^2\ g^{-1}$)	*BJH* pore volume ($cm^3\ g^{-1}$)
CuNiMgAl(OH)$_x$	1.9	98.8	0.97
CuNiMgAlO$_y$	5.9	148.9	1.07

Meanwhile the H_2–N_2O titration studies are also introduced to investigate the state of the surface Cu metal particles. From the results (Fig. 2S in Supplementary material), all H_2 consumption peaks are clearly observed to appear at about 220 °C, which is lower than that for the Cu^{2+} reduction in CuNiMgAlO$_y$ (287 °C, in Fig. 2), indicating that all copper species titrated by N_2O are active particles. And the intensity of H_2 consumption peak decreases with the increasing activation temperature. According to the surface stoichiometry of the titration Cu^0 with N_2O and using the calculation methods reported [5,6], the Cu dispersion (D_{Cu}), the Cu metal specific area and the average Cu^0 particle size (r_{av}) of the catalyts activated by H_2 at above 300 °C have been calculated and the values obtained are shown in Table 2. The results clearly show that the Cu dispersion and metal surface area decrease, however the Cu average particle sizes increase with the increasing activation temperature, indicating that the Cu particles are obviously agglomerated at a high temperature. Moreover the average Cu particle sizes in the reduced catalysts (3–4.5 nm) are much smaller and the D_{Cu}% values are larger than those of the supported catalysts as reported [9,14].

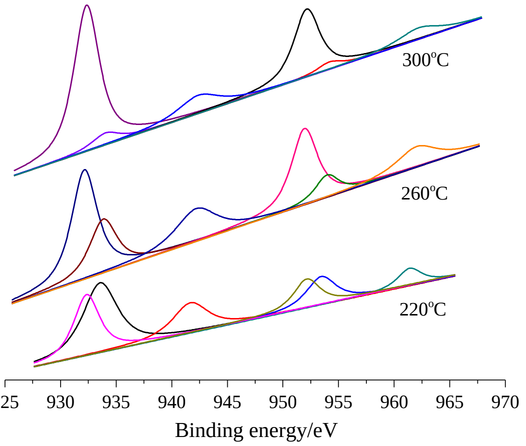

Fig. 3. Cu2p XPS patterns of CuNiMgAlO$_y$ catalyst activated by H_2 at 220, 260 and 300 °C, respectively.

Table 2
Cu dispersion, metal area, and average particle size of the catalysts activated by H_2 at different temperature.[a]

Activation temperature/°C	D_{Cu} %	Cu metal area ($m^2 g^{-1}$-cat)	r_{av}/nm
300	35.84	30.67	2.9
360	29.89	25.58	3.5
400	23.39	20.01	4.5

[a] According to the H_2–N_2O titration.

It shows that the catalysts with highly dispersed catalytic active centers can be obtained from the hydrotalcite-like materials as precursors.

3.3. Catalytic performance

From the catalytic performance of different catalysts in the FFR liquid-phase (ethanolic solution) hydrogenation (Table 3), it is found that $MgAlO_y$ has almost no catalytic activity for the FFR hydrogenation, and $NiMgAlO_y$ or $CuMgAlO_y$ gives above 52% of FFR conversion. However, $NiMgAlO_y$ gives a higher proportion of 2-diethoxylmethxyl-furan (2-DEMF) than $CuMgAlO_y$. According to the H_2-TPR results, it can be deduced that the FFR acetalization [15] easily occurs due to the presence of nickel cations as Lewis acids on the surface. The copper cations will be less acidic and, thus, less efficient to catalyze the acetalization of FFR. Meanwhile, $CuNiMgAlO_y$ gives the highest FFR conversion (90.5%) and the lowest 2-DEMF selectivity, indicating that the Ni^{2+} species have a synergistic effect on the FFR hydrogenation on the Cu^0 active centers in the catalysts.

Fig. 4 shows the results on the FFR liquid-phase hydrogenation over $CuNiMgAlO_y$ catalysts activated by H_2 at different temperatures. There are three main products formed, FFA, 2-methylfuran (2-MF) and 2-diethoxylmethxyl-furan (2-DEMF). FFA arises from FFR hydrogenation and 2-DEMF results from FFA hydrogenolysis. Moreover, both FFR conversion and FFA selectivity clearly increase first and then decrease upon increasing the activation temperature. However, the 2-MF selectivity follows an inverse trend. The highest FFR conversion (90.5%) and FFA selectivity (85.4%) are obtained along with the lowest 2-MF selectivity (4.3%) at 300 °C. It shows that the activation temperature is an important factor affecting the catalytic properties of $CuNiMgAlO_y$ and 300 °C seems to be an optimum activation temperature. According to the XPS and H_2-TPR results, it is also deduced that Cu^0 species are the effective catalytic centers for the FFR hydrogenation, which is in agreement with the previous reports [1,2,12]. From the H_2–N_2O titration results, the decrease on both FFR conversion and FFA selectivity upon increasing the temperature are concluded to be due to the agglomeration of active Cu^0 particles at a high activation temperature, the presence of larger Cu^0 particles favours the FFA hydrogenolysis to 2-MF.

From the FFR vapour-phase hydrogenation over $CuNiMgAlO_y$ (Fig. 5), two other by-products including tetrahydrofurfuralcohol (THFFA) and 2-methyltetrahydrofuran (2-MHF) are found besides the two main products FFA and 2-MF. The two by-products result from the hydrogenation of furan ring of FFA and 2-MF, respectively. When the catalyst activation temperature is raised from 220 to 400 °C, the FFR conversion in the vapour-phase hydrogenation shows a trend similar to that in the liquid-phase hydrogenation, it decreases. This suggests that FFR hydrogenation is inhibited to some extent by the agglomeration of the Cu particles. On the other hand, the selectivities of FFA and 2-MF formation show an inverse trend. Clearly 300 °C is an important break point at which there is change of the trends for FFA and 2-MF selectivities: the FFA selectivity increases from 32% to 80% and the 2-MF selectivity decreases from 48% to 10% between 300 °C and 400 °C. The increase of the FFA selectivity and the decrease of the 2-MF selectivity with the increase of the activation temperature are most probably due to the short contact time of FFR and FFA with the catalytic active centers.

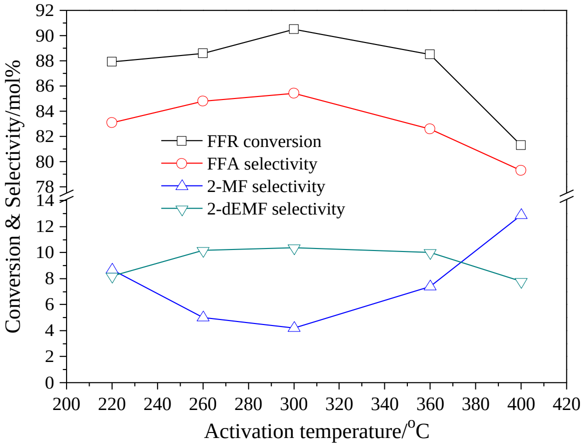

Fig. 4. Effect of the catalyst activation temperature on FFR liquid-phase hydrogenation over $CuNiMgAlO_y$. Conditions: 90 mL ethanol, 30 mL FFR, 1 MPa H_2, 1 g catalyst activated for 2 h, stirring at 500 r min^{-1}, reaction at 200 °C for 2 h.

From the catalytic cycle results (Fig. 3S and 4S in the Supplementary material) of $CuNiMgAlO_y$ activated by H_2 at 300 °C, it is shown that the catalytic activity of $CuNiMgAlO_y$ has no obvious decrease after 3 cycles, and only about 10% decrease on the FFR conversion after 6 cycles in the FFR liquid-phase hydrogenation. And the catalytic properties of $CuNiMgAlO_y$ in vapour-phase hydrogenation stay nearly unchanged after 36 h. This indicates that $CuNiMgAlO_y$ from the hydrotalcite-like precursors exhibits a stable catalytic performance in FFR hydrogenation.

Table 3
Catalytic performance of the different catalysts.[a]

Catalysts	FFR conversion/ mol%	Products distribution/mol%		
		FFA	2-MF	2-dEMF
$MgAlO_y$	9.8	59.8	–	40.2
$NiMgAlO_y$	55.6	53.2	–	46.8
$CuMgAlO_y$	52.7	78.1	8.0	13.9
$CuNiMgAlO_y$	90.5	85.4	4.7	10.1

[a] 1 g catalyst activated by H_2 at 300 °C for 2 h, 90 mL ethanol, 30 mL FFR, 1 MPa H_2, stirring at 500 r min^{-1}, reaction at 200 °C for 2 h.

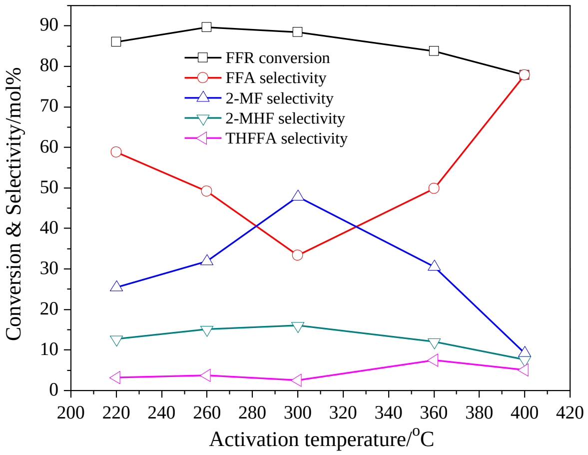

Fig. 5. Effect of the catalyst activation temperature on FFA vapour-phase hydrogenation over $CuNiMgAlO_y$. Conditions: catalysts activated for 2 h, GHSV = 4000 h^{-1}, H_2/FFR molar ratio = 10.1, reaction at 220 °C.

4. Conclusions

In FFR hydrogenation, the catalyst activation temperature is found to be an important factor affecting the dispersion of the active centers of catalysts ($CuNiMgAlO_y$) prepared from the hydrotalcite-like precursors. 300 °C is an optimum activation temperature to obtain the best FFR hydrogenation catalysts with a high Cu dispersion, a large metal specific area and small particle sizes. FFR hydrogenation is inhibited by the agglomeration of active Cu particles. FFA hydrogenolysis to 2-MF easily occurs over the larger Cu particles in FFR liquid-phase hydrogenation (ethanolic solution) and hydrogenation of the furan ring of FFA and 2-MF occurs in the vapour-phase hydrogenation in the absence of ethanol.

Appendix A. Supplementary data

Supplementary data to this article can be found online at doi:10.1016/j.catcom.2011.03.011.

References

[1] B.M. Nagaraja, A.H. Padmasri, B.D. Raju, K.S.R. Rao, J. Mol. Catal. A 265 (2007) 90–97.

[2] B.M. Nagaraja, A.H. Padmasri, P. Seetharamulu, K.H.P. Reddy, B.D. Raju, K.S.R. Rao, J. Mol. Catal. A 278 (2007) 29–37.

[3] J. Lessard, J.F. Morin, J.F. Wehrung, D. Magnin, E. Chornet, Top. Catal. 53 (2010) 1231–1234.

[4] C.X. Chen, C.H. Xu, L.R. Feng, Z.J. Li, J.S. Suo, F.L. Qiu, Adv. Synth. Catal. 347 (2005) 1848–1854.

[5] J.W. Evans, M.S. Wainwright, A.J. Bridgewater, D.J. Yong, Appl. Catal. 7 (1983) 75–83.

[6] E.D. Guerreiro, O.F. Gorriz, J.B. Rivarola, L.A. Arrúa, Appl. Catal. A 165 (1997) 259–271.

[7] Y. Lwin, A.B. Mohamad, Z. Yaakob, W.R. Wan Daud, React. Kinet. Catal. Lett. 70 (2000) 303–310.

[8] F. Kovanda, K. Jirátová, J. Rymeš, D. Koloušek, Appl. Clay Sci. 18 (2001) 71–80.

[9] S.M. Auer, R. Wandeler, U. Göbel, A. Baiker, J. Catal. 169 (1997) 1–12.

[10] S. Albertazzi, F. Basile, P. Benito, P.D. Gallo, Catal. Today 128 (2007) 258–263.

[11] A. Schutz, P. Biloen, J. Solid State Chem. 68 (1987) 360–368.

[12] B.M. Nagaraja, V.S. Kumar, V. Shasikala, A.H. Padmasri, B. Sreedhar, B.D. Raju, K.S.R. Rao, Catal. Commun. 4 (2003) 287–293.

[13] J. Wu, Y.M. Shen, C.H. Liu, H.B. Wang, C.J. Geng, Z.X. Zhang, Catal. Commun. 6 (2005) 633–637.

[14] Z.Y. Ma, C. Yang, W. Wei, W.H. Li, Y.H. Sun, J. Mol. Catal. A 231 (2005) 75–81.

[15] F. Gandara, B. Gomez-Lor, E. Gutierrez-Puebla, Chem. Mater. 20 (2008) 72–76.